IOSR Journal of Applied Geology and Geophysics (IOSR-JAGG)
e-ISSN: 2321–0990, p-ISSN: 2321–0982.Volume 10, Issue 5 Ser. I (Sep. – Oct. 2022), PP 40-48
www.iosrjournals.org

Application of 2-D Electrical Resistivity Tomography and Modeling for Sand Exploration at Evbarue, Edo State, Nigeria

Irunkwor, T. C[1], Eghobamien, L.O[2] and Abanjo, N[3]
[1]*Department of Environmental Management and Toxicology, University of Delta, Agbor, Delta State, Nigeria*
[2]*Rural Water Supply and Safety Department, Edo STRUWASSA, Benin City, Edo State, Nigeria*
[3]*Department of Geology, University of Delta, Agbor, Delta State, Nigeria*

Abstract
Vertical electrical sounding and 2-D electrical resistivity tomography was applied to investigate the availability of sand and estimate the volume of exploitable sand deposit in a municipality in the Western Niger Delta. Vertical electrical sounding (VES) and 2-D resistivity tomography was investigated using the Petrozenith PZ-03 terrameter with the Schlumberger and Wenner arrays respectively. The VES and 2-D resistivity survey results were respectively interpreted with IPI2WIN and DIPROWIN softwares. Resistivity results delineated 3 layers of lateritic topsoil, sandy clay, and sand. The VES and 2-D tomography mapped and identified sand deposits of varying resistivity values ranging from 1362Ωm to 4040Ωm at a depth range of 1.5m to 39.6m. The sand deposit was characterized by medium to coarse grained sand that is moderately sorted. An estimated volume of 867,122m^{3}of sand is available for mining from the 138,912,944 tonnes of sand deposit which is considered sufficient enough to be of economic value. Since mining this volume of sand will have adverse environmental effects on the river micro-ecology and the community, it is advised that conscious steps be taken to minimize ecological and environmental effects, and the river flow be directed away from sensitive and vulnerable banks in order to avoid erosion and bank instability.

Keywords: *2-D Electrical Resistivity Tomography, Sand, Vertical Electrical Sounding, Volume of Exploitable Sand*

Date of Submission: 09-10-2022 Date of Acceptance: 23-10-2022

I. Introduction

Silici-clastic sand which is a non-renewable resource is mainly made up of quartz, natural gas, feldspar and somewhat calcium sulphate such as gypsum and selenite. It is an indispensible naturally occurring aggregate resource for any society due to the great impact it has on the quality of lives of humans in water filtration, in painting, for the production of blocks, bricks, pipes, for land reclamation, for mortar, shale gas extraction and beach renourishment programmes. Sand deposits are good groundwater and hydrocarbon reservoirs. They are also sources of obtaining economic placier deposits such as gold, tin, diamond, etc and are useful construction aggregates for civil engineering works such as airports, bridges, roads, highways, residential and commercial buildings, power generating facilities, factories, water supply and waste treatment facilities (Okiongbo and Soronnadi-Ononiwu, 2018). Sand is a natural resource that is used to make glass, roofing shingles, on icy roads in the winter, for asphalt, for railroad ballast and as an abrasive to make concrete. Since it will be difficult for humans to maintain the current quality of life without sand, it is therefore mined or explored to meet up with these various activities by man.

Sand is extracted in various areas from open pit, beaches, inland dunes, river beds, ocean beds and along river channels in the Niger Delta. As sand is extracted rapidly, groundwater evaporates fast reducing groundwater recharge, increasing the failure of irrigation, wells, and the associated predicament in farming (Kelly, 1977). Sand mining has been attributed to the direct cause of erosion which destroys farmlands and local wide life (Eteh *et. al.*, 2021).

To search for sand and investigate whether it is of economic value to explore, the electrical resistivity technique is employed since it has been used as a viable tool for locating and mapping sand and gravel deposits by Wilcox (1932), Jakosky (1950) and Welkie and Meyer (1983). This geophysical exploration technique has also been used in recent times by Haeni (1995) and Nowroozi *et. al*. (1997) to investigate hydrological, geotechnical, engineering and environmental problems. The electrical resistivity method has been used for hydrogeological investigations in the Niger Delta (Okiongbo and Mebine, 2015; Okiongbo and Akpofure, 2016) and in the exploration of shallow alluvial aquifer all over the world (Umar *et. al.*, 2006). In these studies, the electrical resistivity has proven its usefulness as a qualitative indicator that displays good resistivity contrasts between the overburden, sand and bedrock. The electrical resistivity technique has been used to delineate compositional variations in a rock layer in the subsurface and can therefore be used to distinguish between different geological sequences like clean sand that has high resistivity signature and clay with low resistivity signature. If the fluid conductivity does not vary, the resistivity of unconsolidated sedimentary deposits generally increases with grain size and the electrical resistivity method is capable of providing a qualitative estimate of the grain size of a sand deposit (Urish, 1981; Haeni, 1995). The applicability of electrical resistivity method to sand exploration is dependent on the high resistivity contrast between coarse grained materials and the host/surrounding rock, soil, clay or silt.

Borehole records from the works of Akpokodje and Etu-Efeotor (1987) and Okiongbo and Soronnadi-Ononiwu (2018) shows a wide occurrence of sand in the Niger Delta and the sand deposits are usually overlain by clayey sand or peaty clay that vary from less than 1 to 10m thick whose boundaries are usually sharp but may be occasionally gradational. Arising from the increase in population in the Niger Delta, there is a corresponding increase in the demand for sand for domestic and industrial purposes. This has necessitated the need for detailed geological information of any site that is considered for dredging so as to investigate if the promising potential and exploitable volume of sand in the area is of economic value. This study was therefore aimed at determining the availability of sand, estimate the strippable overburden and to effectively map the lithology and areal extent of the volume of exploitable sand deposit at Evbarue community of Edo State using the vertical electrical sounding (VES) and 2D resistivity imaging technique.

II. The Study Area

2.1 Regional Geology and Topography

The study area, Evbarue community, has border with one of the tributaries of Ikpe (Ossiomo) River in Orhionmwon Local Government Area of Edo State, Nigeria. It lies within Latitude 06^0 12.89’ and 06^o13.3’ North of the Equator and Longitude 005^0 46.11’ and 005^o46.40’ East of the Greenwich Meridian (Figure 1). The geological structure of the region (Edo State) comprises crystalline basement rocks in the Northern part which is Precambrian in age and the sedimentary rocks that are ubiquitous in the southern part which is Cretaceous to Recent in age (Allen, 1965). The study area is underlain by the *Benin Formation* often referred to as *the Coastal Plain Sands* of the lower Quaternary period and Pliocene-Pleistocene epoch (Figure 2). The inclusive Aluvium belongs to the upper Quaternary (Recent Sediments) and consists of silty-clayey sands, sands and gravels (Short and Stauble, 1965). The geomorphology of the area is relatively flat lying to steep with both marine and fluvial sediments.

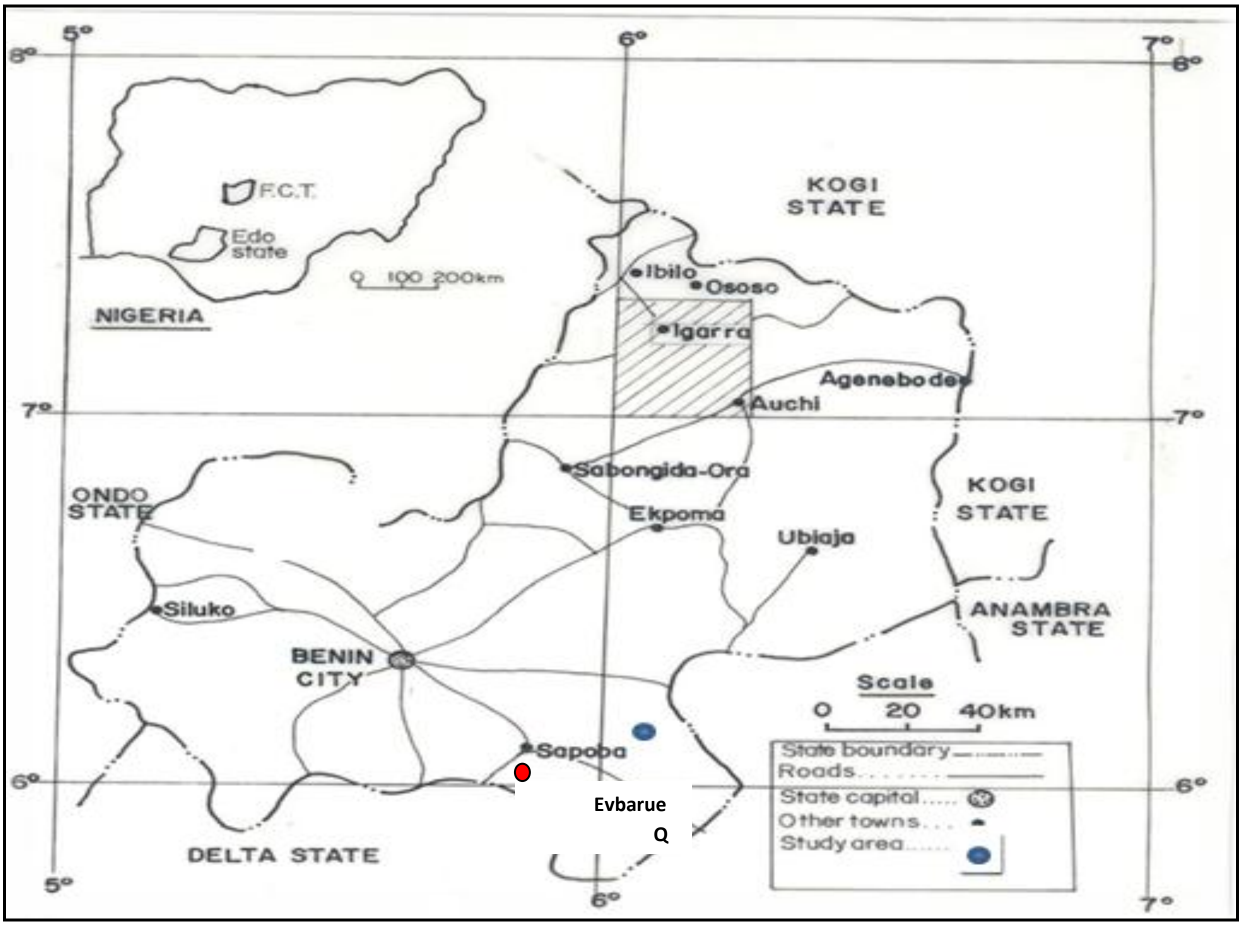

Figure 1: Map of Edo State Showing the Study Area (SW of Benin City)

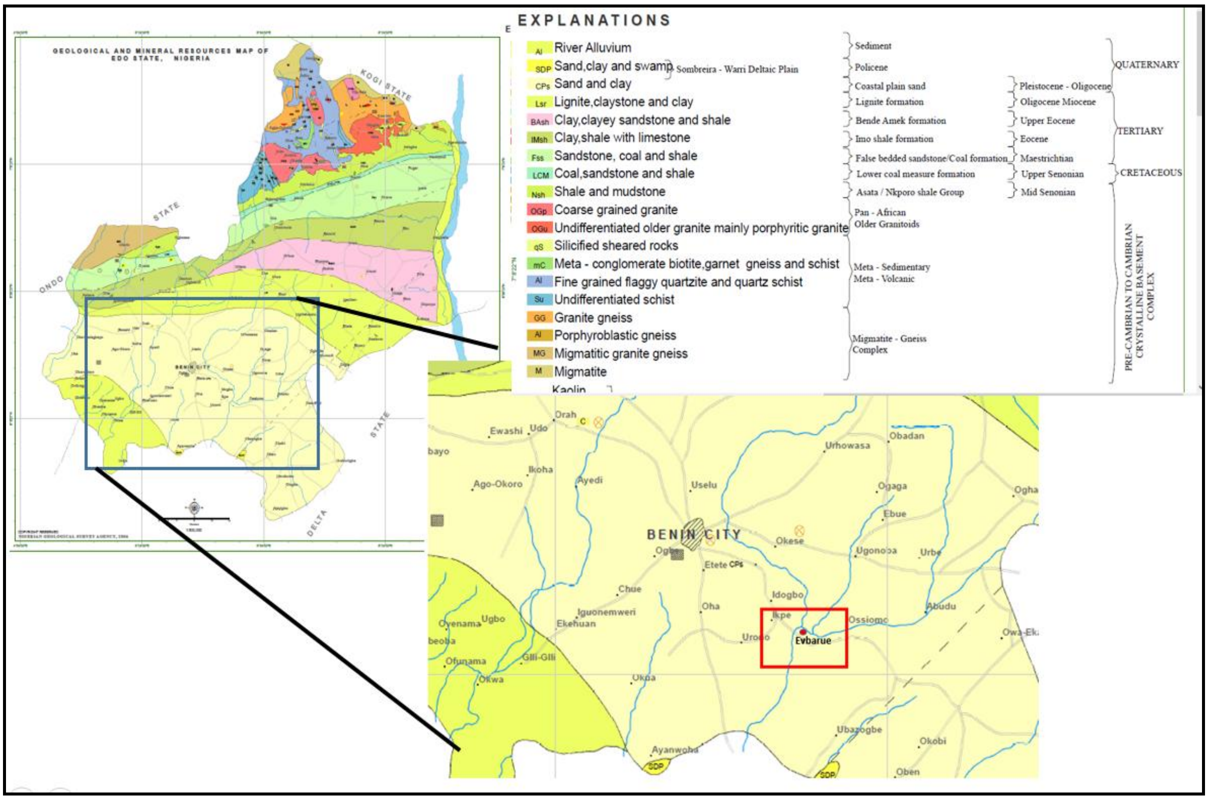

Figure 2: Geologic Map of Edo State showing the Study Area in Red Box (SE of Benin City)

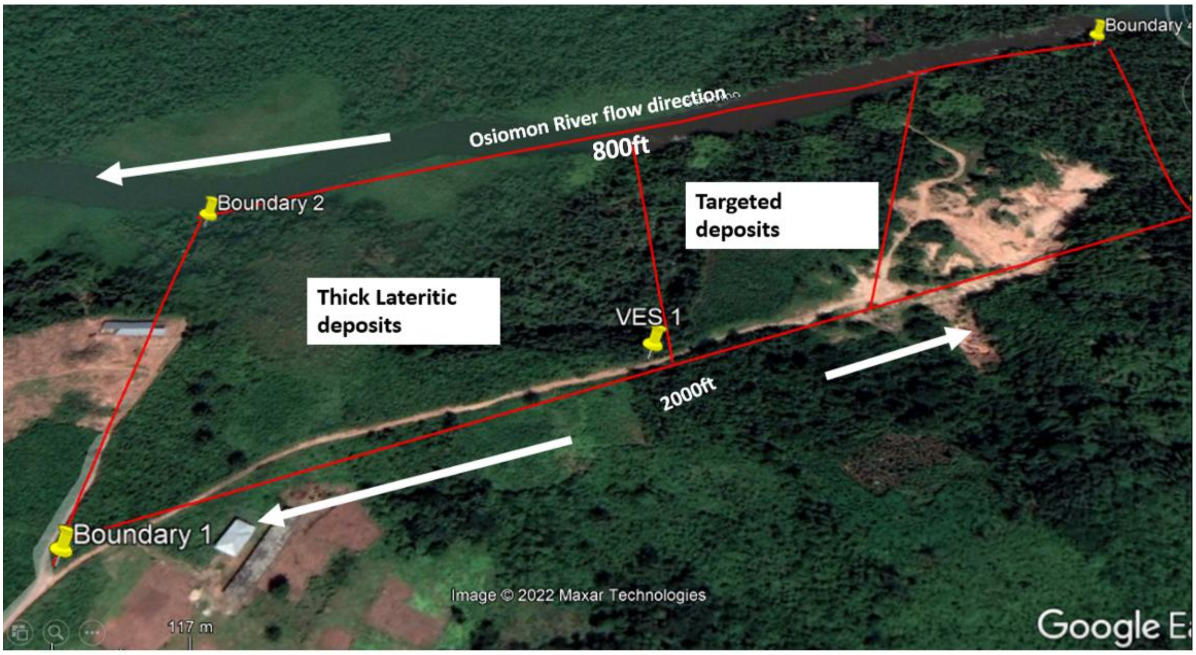

Figure 3: Trapezoidal Shape of the Surveyed Area with River Ossiomo flowing South West

III. Material and Methods

3.1 Data Acquisition

The electrical resistivity method involves injecting current into the subsurface via two current electrodes, AB and the potential difference created due to the passage of the electric current through the earth materials is measured across a pair of potential electrodes, MN. The Schlumberger and Wenner arrays were employed for the survey. The data for both the vertical electrical sounding (VES) and 2-D resistivity imaging was acquired using the *Petrozenith PZ-03* Terrameter where consecutive readings are taken automatically and the results are averaged continuously. The continuously updated running average is displayed as resistance automatically.

3.2 Vertical Electrical Sounding

The vertical electrical sounding (VES) was run in the NE-SW direction. A maximum current electrode expansion (AB/2) of 150m and potential electrode expansion (MN/2) of 10m was utilized using Schlumberger array because it is faster, more economical to use and less sensitive to lateral variation. For each resistivity station where measurement was made, a reading of resistance R of the volume of the earth material within the electrical space of the electrode configuration was obtained. The measured resistance values (R) were converted into apparent resistivity (ρ_a) by multiplying with a geometric factor (K), such that:

$$\rho a = \pi R \frac{[(AB/2)^2-(MN/2)^2]}{MN} = \pi RK \quad \ldots (1)$$

Where K is the geometric factor and is given by:

$$\frac{(AB/2)^2-(MN/2)^2}{MN} \quad \ldots (2)$$

The obtained apparent resistivity values were used to generate sounding curves which were interpreted qualitatively and quantitatively. Quantitative interpretation of the curve was by partial curve matching and computer iteration techniques using the 1-D inversion IPI2WIN software to obtain geoelectric section of the one-dimensional resistivity model for the area. This software uses least-squares optimization technique in which a starting model is adjusted successively until the difference between the field data and the model output is reduced to a minimum. The software also converts the apparent resistivities obtained as a function of spacing in the field to true resistivities as function of depth. Although in constructing a model the interpreter arbitrarily divides the subsurface into number of horizontal layers of given thickness, the IPI2WIN software iteratively changes the resistivities in order to obtain a best fit with the field data for the layer thicknesses chosen for the model. The resulting true resistivities represent the best average bulk resistivity for the given layer.

3.3 2-D Resistivity Imaging

The 2-D resistivity profile was run using the Wenner array. The resistivity imaging acquired was to complement the 1-D geoelectrical sounding data because it displays a clearer picture of the lateral and vertical variation of the subsurface lithology. Each of the 2-D transverses was 180m in length. The electrode spacing ranged from 10 to 60m in an interval of 10m, with a total of 18 electrode positions for the transverse line. The profile lines are in NE-SW direction. The electrodes are laid in a straight line with 'a' spacing of 10m between consecutive electrodes, where C_1 and C_2 are current electrodes and P_1 and P_2 are potential electrodes. After the set up, the first reading was taken at the first station thereafter the cables were moved to the next position being electrodes 2, 3, 4 and 5 which are used for C_1, P_1, P_2, C_2 respectively. This is repeated down the line until electrodes 15, 16, 17 and 18 were used for the last measurement with '1a' spacing. For the 18 electrodes, there are 15 possible measurements with 10m spacing for the wenner array.

After completing the sequence, the next measurements with 10m spacing using the 20m electrode spacing is made where electrodes 1, 3, 5 and 7 were used for the first measurement and electrodes 2, 4, 6 and 8 are used for the second measurement. This method was repeated down the line until electrodes 12, 14, 16 and 18 was used for the last measurement. The same process was repeated for measurements of 30m, 40m, 50m and 60m. The resistivity profiling data were processed using an iterative constrained least square inversion method to create a model of subsurface resistivity by inverting the apparent resistivity data. The DIPROWIN software was used which is 2-D resistivity and IP inversion programme for interpretation of resistivity data employing the mathematical Jacobian rule modeling (Loke and Barker, 1996). The computer programme automatically subdivides the subsurface into number of blocks, and then uses least-squares smoothness constrained inversion scheme to determine the appropriate resistivity value for each block. The 2-D DIPROWIN software carries out an inversion of the data and presents the result in contouring format reflecting qualitatively the spatial variation in resistivity with depth. The contoured data can be modeled using a 2-D finite or finite difference algorithm (Griffiths and Barker, 1993; Ugwu *et. al.,* 2016). The measured resistance values (R) were converted into apparent resistivity (ρ_a) by applying the formula:

$$\rho a = 2\pi aR \quad \text{…} \quad (3)$$

Where a = distance between adjacent electrodes (m), and π = Constant = 3.142.

IV. Results and Discussion

4.1 VES Data Results

The result of the 1-D resistivity survey and the K-type curve is shown in Figure 4. The apparent resistivity values and the corresponding lithology of the 3 delineated layers of lateritic topsoil, sandy clay and sand are presented in Table 1. The apparent resistivity values obtained for the three delineated layers of the 1-D inversion model varied from 138.2 Ω-m to 300.7 Ω-m to a depth of 1.34m for the first layer, 2159 Ω-m to 4705 Ω-m to a depth of 15.20m for the second layer, and 1413 Ω-m to 4022 Ω-m to a depth of 53.30m for the third layer. The thickness of the layers ranged from 0.6m to 1.34m for the first layer, 1.34m to 15.20m for the second layer and 15.20m to 53.30m for the third layer. The VES revealed K-type curve which implies that resistivity decreases at shallow depths but increases as depth increases thus signifying a possible indicator of the presence of aggregate materials such as sand. Since authors like Baines *et. al.* (2002), Beresnev *et. al.* (2002) and Magnusson *et. al.* (2010) adduced that the potential sand deposits are easily distinguished by their high resistivity values from their surrounding clay and silt, the basal unit underlying the sandy clay layer in this study which exhibits high resistivity is the supposed major targeted unit for the sand production. The VES result therefore showed that the lateritic topsoil and the underlying sandy clay layer to a depth of 15.20m (or about 16m) must be excavated in order to access the targeted sand deposit. Thus, a thickness of 15.20m which comprises the thickness of the lateritic topsoil and the sandy clay layer constitute the strippable overburden that must have to be excavated to access the sand deposit. It also revealed that the thickness of the sand deposit is 38.1m (ie 18.5m +19.6m).

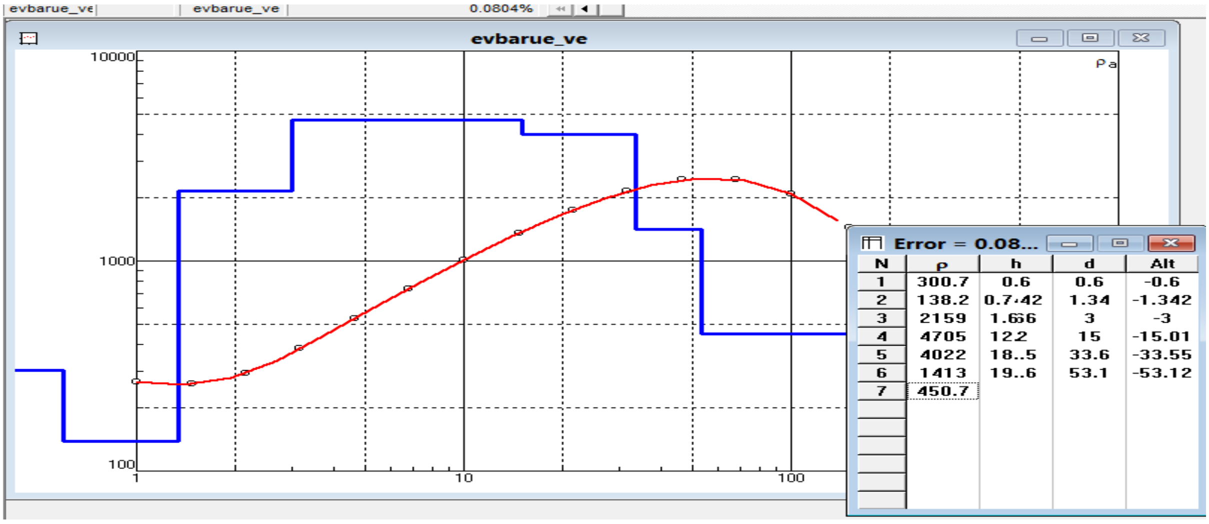

Figure 4: Field Curve of the 1-D resistivity model

Table 1: Lithologic Delineation and Curve type of the 1D Inversion Model from the VES Station

Location	Layer	Resistivity (Ωm)	Thickness(m)	Depth(m)	Lithology	Curve Type
EVBARUE COMMUNITY	1	300.70	0.600	0.600	**Lateritic Top Soil**	$\rho_1<\rho_2>\rho_3$
		138.20	0.742	1.342		
	2	2159.00	1.660	3.002	**Sandy Clay**	K
		4705.00	12.200	15.202		
	3	4022.00	18.500	33.702	**Sand**	
		1413.00	19.600	53.302		
	4	450.70	-	-	**Sandy Clay**	

4.2 2-D Resistivity Imaging Data Results

The earth model of 2-D resistivity imaging which was run to corroborate with the VES is shown in figures 5 to 7. The result revealed that the lateritic topsoil resistivity varied from 89 Ω-m to 385 Ω-m to a depth ranging from 0.6m to 3.20m at a lateral distance of between 15m to 29m. The resistivity of the sandy clay layer varied from 459 Ω-m to 134 Ω-m to a depth ranging from 3.20m to 24.9m, while the resistivity of the sand layer varied from 1362 Ω-m to 4041 Ω-m to a depth ranging from 8m to 39.6m at a lateral distance of between 15m to 140m. It was also shown in figures 5 to 7 that the upper section of the surveyed area has high degree of ferrugenised topsoil whose thickness increases towards the boundary at the beginning of the mapped area of 13.73m (45ft) thick, but thins out in thickness to about 1.5m (5ft) towards the distal or low-lying area of the site. The 2-D imaging showed that the sand deposit is characterized by medium to coarse grained sand that is moderately sorted with high maturity in mineralogy of about 95% quartz, 2% clay mineral and 2% specs of iron III oxide.

4.3 Estimation of Available and Dredgeable Volume of Sand

To estimate the available and dredgeable volume of sand deposit in the area, the shape of the surveyed area was considered. The shape of the surveyed area is trapezoidal (Figure 3) where the top (L_1) and bottom (L_2) lengths are respectively 244m (800ft) and 610m (2000ft). The total depth of the surveyed area extracted from the VES data was 53.30m. The thickness of the dredgeable sand column from the VES result is 18.5m + 19.6m = 38.1m which are the same from the 2-D resistivity imaging result (ie 39.6m – 1.5m = 38.1m).

Volume of Trapezium (Volume of available dredgeable sand) = Area of trapezium x thickness

= ½ (L_1+L_2) x depth x thickness

= ½(244+610) x 53.30x 38.10

Volume of Trapezium (Volume of available dredgeable sand) = **867,121.71m^3 ≈ 867,122m^3**

The mass of this dredgeable sand occupying the study area was also estimated as follows:

Mass of dredgeable sand = Density of sand x Volume of sand

But density of sand = 1.602g/cm^3 = 1602kg/m^3

Thus:

Mass of Dredgeable Sand = 1602 x 867,122 = **1,389,129,444kg or 138,912,944 tonnes**.

The estimated volume of available dredgeable sand is 867,122m^3 while the mass of sand deposit in the surveyed area is 138,912,944 tonnes. It should however be noted that when this volume of sand is mined, it is presumed that the flow dynamics of the area will be altered which will exert some adverse impact on the river micro-ecology on sections of the river and the community.

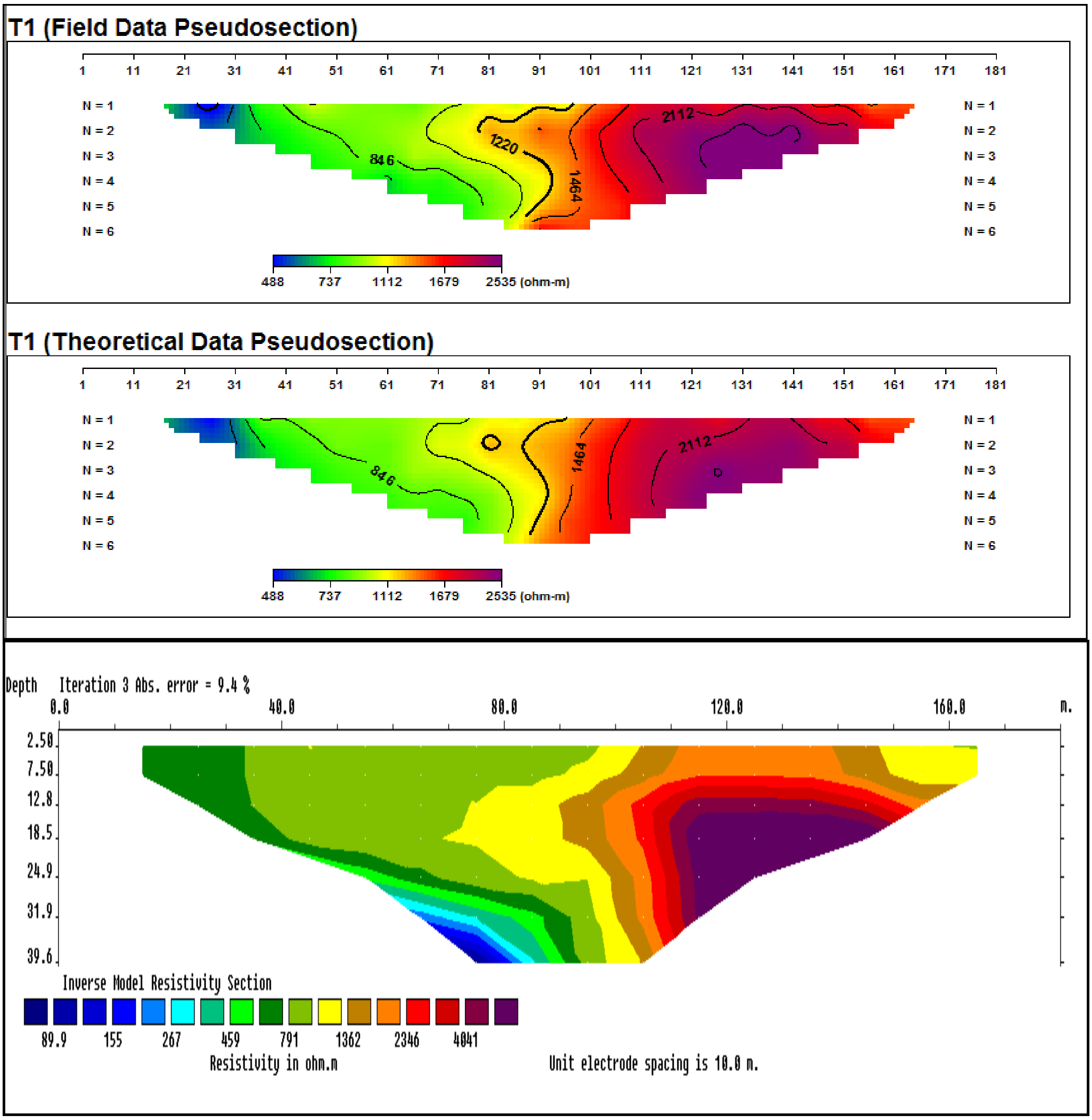

Figure 5: Inverse Model of 2-D Resistivity Pseudosection of the surveyed area

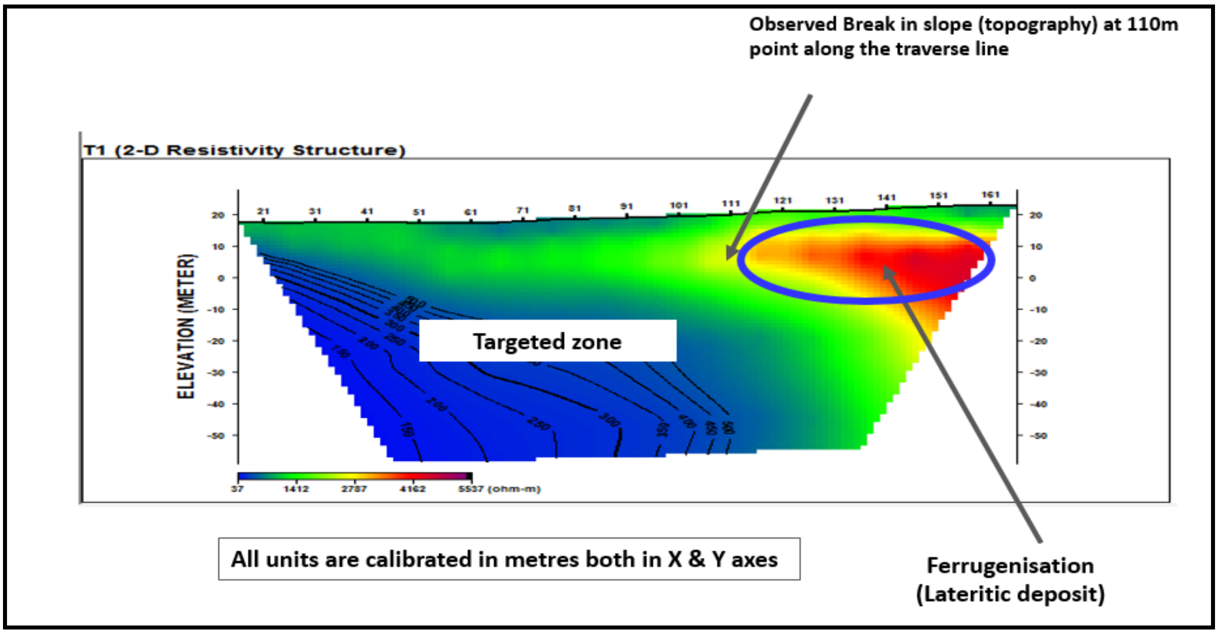

Figure 6: Earth Model of the 2-D Electrical Resistivity Tomography

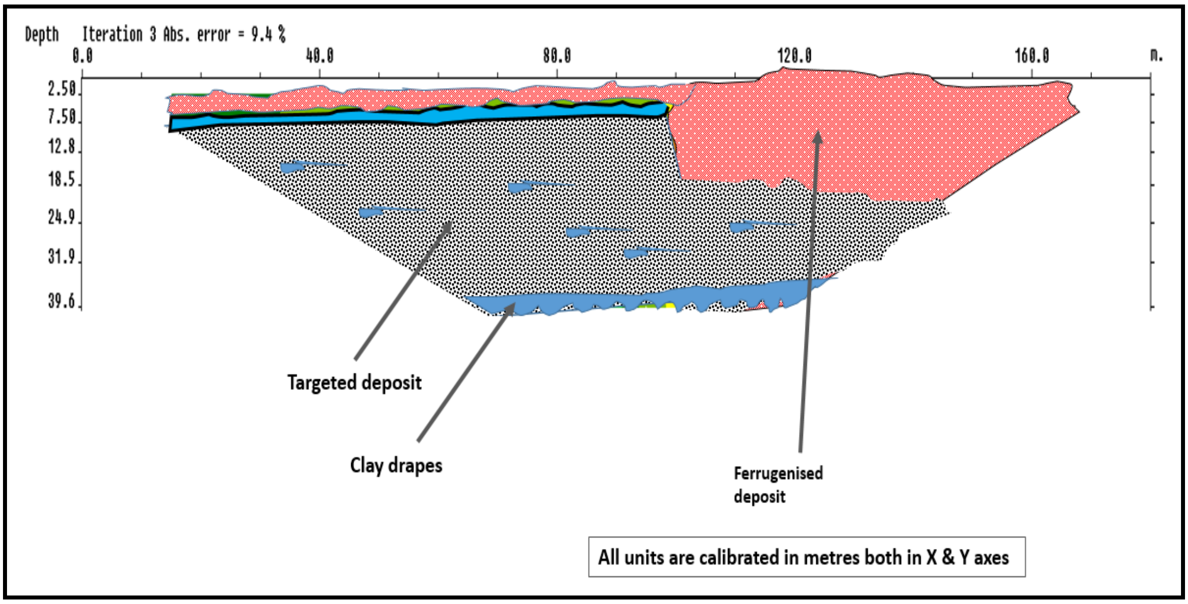

Figure 7: Realized Earth Model of the surveyed Area

V. Conclusion

The study has shown the successful combination of vertical electrical sounding and 2-D electrical resistivity tomography using the Schlumberger and Wenner arrays respectively to map potential aggregate sources in the exploration of sand in Evbarue community so as to determine if the volume of sand is of economic value. The inversion of the geoelectric parameters of both the VES and wenner indicate the presence of sand layer deposit located at depth beyond 15.20m. Arising from the problem of equivalence and suppression in geoelectric sounding data, a very high resistivity contrast occurred at the sandy clay and sand boundary layer but beyond this boundary the layer exhibited a very high resistivity which is a possible indicator of potential sand deposit. The areal extent of the 2-D profiles that was run in trapezoidal shaped survey area was used to estimate the volume and mass of available sand which is respectively 867,122m^3 and 138,912,944 tonnes. This result shows that the sand layer/deposit are characterized by good lateral continuity which is sufficiently thick enough (38.10m) for commercial exploitation therefore can be dredged economically for domestic and construction purposes. However, mining this volume of sand will have adverse environmental effects on the river micro-ecology on sections of the river and the community. It is therefore recommended that conscious steps be taken to minimize ecological and environmental effects, and the river flow be directed away from sensitive and vulnerable banks in order to avoid erosion and bank instability.

Acknowledgment

The authors sincerely acknowledge the management and staff of Ligaliz Geophysical Enterprise for the acquisition of data.

References

[1]. Akpokodje, E. U. and Etu-Efeotor, J. O. (1987). The occurrence and Economic potential of clean sand deposits of the Niger Delta. *Journal of African Earth Science*, 6: 61-65.

[2]. Allen, J. R. L. (1965). Late Quaternary Niger Delta and Adjacent Areas: Sedimentary Environments and Lithofacies. *American Association of Petroleum Geologists Bulletin*, 49(5): 150-167

[3]. Baines, D., Smith, D. G., Frose, D. G., Bauman, P. and Nimack, G. (2002). Electrical Resistivity ground imaging (ERGI): a new tool for mapping the lithology and geometry of channel-belts and valley-fills. *Sedimentology*, 49: 441-449.

[4]. Beresnev, I. A., Hruby, C. E. and Davis, C. A. (2002). The use of multi-electrode resistivity imaging in gravel prospecting. *Journal of Applied Geophysics*, 49: 245-254.

[5]. Eteh, D. R., Omonefe, F. and Ejaita, E. (2021). Estimation of Volume of Sand Using Vertical Electrical Resistivity Imaging: A Case Study in Tombia, Yenagoa, Bayelsa State, Nigeria. *United Nations International Journal for Research and Technology*, 2(12): 79-84.

[6]. Griffiths, D. H. and Barker, R. D. (1993). Two-dimensional resistivity imaging and modeling in areas of complex geology. *Journal of Applied Geophysics*, 20: 211-226.

[7]. Haeni, F. P. (1995). Application of Surface-geophysical methods to investigations of sand and gravel aquifers in the glaciated north eastern United States. Regional Aquifer-System Analysis-Northeast Glacial Valleys. United States Geological Survey Paper, A1-A70.

[8]. Jakosky, J. J. (1950). *Exploration Geophysics*. 2nd Edition. Los Angeles: trija Publishers.

[9]. Kelly, W. (1977). Geoelectric Sounding for Estimating Aquifer Hydraulic Conductivity *Groundwater*, 15(6): 420-424.

[10]. Loke, M. H. and Barker, R. D. (1996). Rapid Least-squares inversion of Apparent Resistivity Pseudosections using a Quasi-Newton Method. *Geophysical Prospecting*, 44(1): 131-152.

[11]. Magnusson, M. K., Fernlund, J. M. R. and Dahlin, T. (2010). Geoelectrical imaging in the Interpretation of geological conditions affecting quarry operations. *Bulletin of Engineering Geology and Environment*, 69: 465-486.

[12]. Nowroozi, A. A., Whittecar, G. R. and Daniel, J. C. (1997). Estimating the yield of crushable stone in an alluvial fan deposit by electrical resistivity methods near Stuart Draft, Virginia. *Journal of Applied Geophysics*, 38: 25-40.

[13]. Okiongbo, K. S. and Mebine, P. (2015). Estimation of aquifer hydraulic parameters from geoelectric method-A case study of Yenagoa and environs, Southern Nigeria. *Arabian Journal of Geosciences*, 8: 6085-6093.

[14]. Okiongbo, K. S. and Akpofure, E. (2016). Hydrogeophysical Characterization of Shallow unconsolidated Alluvial Aquifer in Yenagoa and Environs, Southern Nigeria. *Arabian Journal of Science and Engineering*, 41: 2261-2270.

[15]. Okiongbo, K. S. and Soronnadi-Ononiwu, C. (2018). Characterizing aggregate deposits using electrical resistivity method: case history of sand search in the Niger Delta, Nigeria. *Journal of Earth Sciences and Geotechnical Engineering*, 8(4): 1-16

[16]. Short, K. and Stauble, A. J. (1965). Outline of Geology of Niger Delta. *American Association of Petroleum Geologists*, 51(5): 761-779.

[17]. Ugwu, S. A., Nwankwoala, H. O. and Worlu, S. N. (2016). 2-D Resistivity Imaging and Modeling of a dumpsite in Eneka, Rivers State, Nigeria. *Issues in Scientific Research*, 1(3): 37-44.

[18]. Umar, H., Rahman, Y., Abdul, R. S. and Mohd, S. A. (2006). Determination of Groundwater Aquifer and Marine Clay Layer of the Alluvial Quaternary Deposits of Beruas and Bula Formation. *Geophysics*, 5(3): 6-24.

[19]. Urish, D. W. (1981). Electrical resistivity-hydraulic conductivity relationships in glacial outwash aquifers. *Water Resources Research*, 17: 1401-1408.

[20]. Welkie, C. J. and Meyer, R. P. (1983). Geophysical evidence that the Haeger Till Member underlies Southern western Lake Michigan. *Geoscience Wisconsin*, 8: 45-48.

[21]. Wilcox, S. W. (1932). Sand and gravel prospecting by the earth resistivity method. *Geophysics*, 13: 36-46.

Irunkwor, T. C, et. al. "Application of 2-D Electrical Resistivity Tomography and Modeling for Sand Exploration at Evbarue, Edo State, Nigeria." *IOSR Journal of Applied Geology and Geophysics (IOSR-JAGG)*, 10(5), 2022, pp. 40-48.